thermal conductivity of water in the critical range," Vses. Teplotekh. Inst., Rep. No. 68076091, Moscow (1968).
3. H. Poltz, J. Heat Mass Transfer, 8, 515-522 (1965).
4. H. Poltz and R. Jugel, J. Heat Mass Transfer, 10, 1075-1082 (1967).
5. V. N. Andrianov, Principles of Radiative and Combined Heat Transfer [in Russian], Moscow–Leningrad (1972).
6. N. B. Vargaftik, A. A. Filippov, E. E. Tarzimanov, and E. E. Totskii, Thermal Conductivity of Liquids and Gases [in Russian], Moscow (1978).
7. V. S. El'darov, "Experimental investigation of the thermal conductivity of aqueous solutions of salts as a function of concentration, temperature, and pressure," Author's abstract of dissertation for degree in engineering sciences, Baku (1982).
8. G. A. Safronov, "Thermal conductivity of aqueous solutions," Author's abstract of dissertation for degree in engineering sciences, Baku (1985).

STUDY OF POROUS-SUBLIMATIONAL COOLING

V. V. Druzhinets, N. M. Levchenko, and S. M. Ostroumov

UDC 536.422

A nonmonotonic change in the temperature of the cooled surface and a nonmonotonic increase in the heat-transfer coefficient with an increase in the thermal load are observed in porous-sublimational cooling, and an explanation is offered for these events. The theory is compared with experimental data.

Porous-sublimational cooling [1-3] has several advantages over other methods of cooling that use solid cryogens [4]. Porous-sublimational cooling makes it possible to avoid using mechanical devices to press the solid cryogen to the surface being cooled by contact cooling [4]. This appreciably simplifies the design of the cooling unit and improves the reliability of cryosublimation systems. Experiments in [2] showed that heat transfer between the cryogen and the object being cooled is considerably more intense in porous-sublimational cooling than in other types of cooling which employ solid cryogens. However, the authors of [2] used a porous body composed of copper grids. Here, the thermal conductivity of the porous skeleton of the body was relatively low, and its thermal contact with the surface being cooled was unsatisfactory. In addition, the fact that the temperature and pressure fields in the body were not unidimensional made it impossible to compare the theory [1-3] with the experiment [2].

1. Description of Experiment. In the present investigation, we study the accumulation and sublimation of a solid cryogen in a porous specimen 1 (Fig. 1) having a porosity ε_s = 0.62. The specimen was obtained by sintering powdered copper of grade PMS-N (GOST 460-75). The cylindrical porous specimen 1 was sintered with a disk 2 of monolithic copper containing a sensor 3 (germanium thermal converter) to measure the temperature of the surface 4 being cooled. Mounted on the disk 2 is an electric heater 5 made of a constantin wire connected to a stabilized current source. The foam plastic housing 6 provides thermal insulation from the surrounding cryogen 7, the temperature of which T_L is measured with sensor 8. The lateral surface of the specimen 1 is impermeable to gases (being coated with a layer of vacuum lubricant), so the vapor from the cryogen can leave only through the evacuation surface 9. The entire cold accumulator (Fig. 1) is placed in a transparent cryostat connected to an AVZ-20D vacuum pump. Measurements of the temperatures and power of the heater were made automatically with an SM-4 computer [2, 5].

Experiments were conducted in the following manner. Liquid cryogen (nitrogen or hydrogen) was poured into the cavity of the cryostat so that the cold accumulator (Fig. 1) would be "frozen" into the solid state after solidification of the liquid. We then pumped out the

Physico-Chemical Institute of Low Temperatures, Academy of Sciences of the Ukrainian SSR, Kharkov. Translated from Inzhenerno-fizicheskii Zhurnal, Vol. 60, No. 5, pp. 747-753, May, 1991. Original article submitted April 4, 1990.

 0022-0841/91/6005-0566$12.50

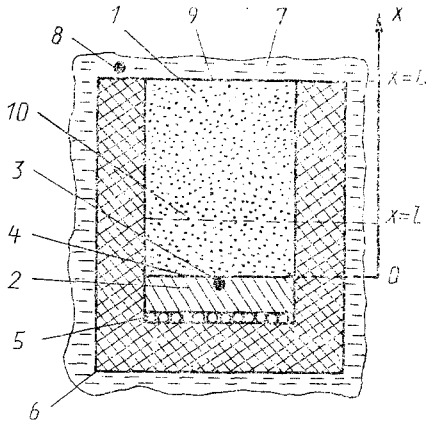

Fig. 1. Sketch of porous-sublimational cold accumulator: 1) porous copper; 2) solid copper disk; 3, 8) heat sensors; 4) cooled surface; 5) electric heater; 6) foam plastic housing; 7) solid cryogen; 9) vapor evacuation surface; 10) sublimation front.

vapor, the rate of evacuation having been chosen so as to avoid any visible drop entrainment during boiling of the liquid or "swelling" of the cryogen after formation of the layer of solid phase. The highest pumping rate was reached at the end of the freezing process. Here, the temperature of the cryogen dropped to a minimum. We then connected the heater and measured temperature and heat input during the sublimation process. The end of sublimation $t = \tau$ was determined from the drop in the temperature of the cryogen and the sharp increase in the temperature of the cooled surface (Fig. 2a for $q_0 = 4382$ W/m^2 and Fig. 2b for $q_0 = 2438$ W/m^2). We then turned off the heater and the vacuum pump, sent a new batch of liquid cryogen into the cryostat, and began the next experiment. The results of the experiments are shown in Fig. 2.

2. Calculation of the Temperature of the Cooled Surface. Since the lateral surface of porous cylindrical body 1 (Fig. 1) is gas-impermeable and thermally insulated and since the pressure P_L and heat flux q_0 are independent of the coordinates, the flow of vapor should be directed along the x axis and flow velocity, temperature, and pressure should depend only on x and t. In this case, porous-sublimational cooling involves the formation of a plane sublimation front $x = \ell(t)$ which moves toward the surface being cooled [1]. The temperature of this front $T_0(t)$ is determined by solving the following system of equations [1] for $\ell(t)$, $T_\ell(t)$, and $T(x, t)$:

$$l(t) = L - \frac{1}{\rho_1 \varepsilon_s s_d \gamma} \int_0^t q_0(z)\, dz, \tag{1}$$

$$P_s^2(T_l) = P_L^2(t) + \frac{2}{\omega k_s} q_0(t)\, \Psi(T_l)\, |L - l(t)|, \tag{2}$$

$$\frac{\partial T}{\partial x} = -\frac{q_0(t)}{\lambda_s(T)}, \quad T|_{x=l} = T_l(t), \tag{3}$$

$$T_0(t) = T(0, t), \quad \Psi(T) = T\eta_2(T), \quad \omega = \gamma\mu/R, \quad \lambda_s(T) = \nu\lambda_{s0}(T).$$

This system of equations describes a process in which heat is removed from the surface being cooled $x = 0$ through the porous skeleton to the sublimation front $x = \ell$. The vapor formed at the front moves through the skeleton toward the evacuation surface $x = L$. Equation (1) reflects the mass balance of the solid cryogen in the region $x < \ell$. Equation (2) follows from Darcy's law and describes the filtration of vapor in the region $x > \ell$ where there is no solid cryogen. The temperature of the vapor in this region $T_2 = T_\ell$, while its density $\rho_2 = \mu P/(RT_\ell)$ [1]. The temperature distribution in the region $x < \ell$ is given by the Fourier law (3). This law accounts for the fact that heat is transmitted mainly through the porous skeleton [1].

In order to solve system (1-3), it is necessary to determine the parameters ε_d, ν, and

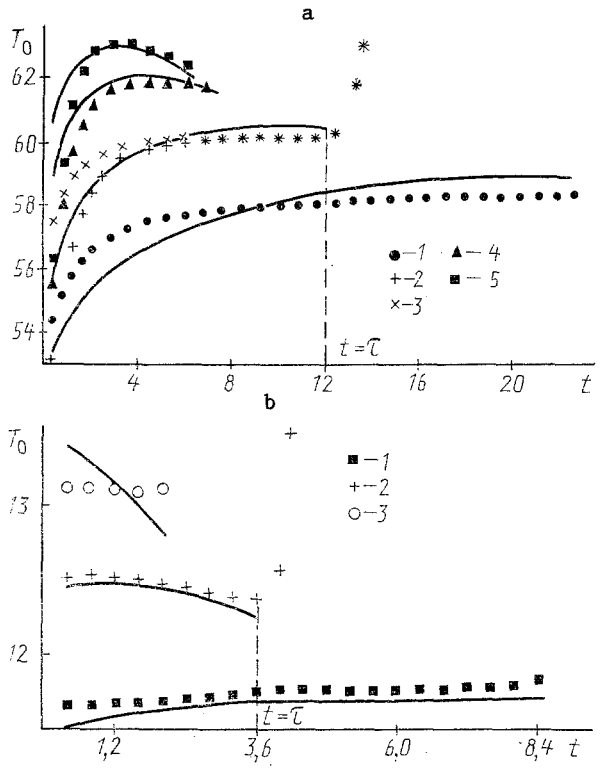

Fig. 2. Temperature T_0 of cooled surface in relation to time t during the sublimation of nitrogen (a) and hydrogen (b) in porous copper: a) 1) q_0 = 2447 W/m^2; 2, 3) 4382; 4) 6843; 5) 8300; b: 1) q_0 = 1074 W/m^2; 2) 2438; 3) 4375; lines show calculated results. T_0, K; t, 10^2 sec.

k_s. The quantity ε_d was calculated from the formula $\varepsilon_d = q_0\tau/(\rho_1\varepsilon_s\gamma L)$, which follows from (1) with q_0 = const and $\ell(\tau) = 0$. The values of q_0 and τ were determined experimentally (see Part 1). For the method of obtaining solid nitrogen and hydrogen described in Part 1, we obtained ε_d = 0.7-0.8. To determine the effective thermal conductivity of the porous body $\lambda_s = \nu\lambda_3$, we performed numerical calculations of $T_0(t)$ for the heating of the porous body with the cryogen. The calculations were performed by the method described in [6], where the disk 2 (Fig. 1) and the porous body 1 were modeled by arcs of a rigid-body curve having a common vertex (surface 4) with the temperature $T_0(t)$. The calculated results were compared with measurements of the temperature of the surface 4 during heating of the body 1 and disk 2 in the evacuated cryostat when there was no cryogen inside or outside the body. The theoretical and experimental values of $T_0(t)$ coincide within the measurement error for ν = 0.1. We subsequently used assigned values of ε_d and ν to solve system (1-3) by a numerical method [1], i.e., we performed calculations of $T_0(t)$ in which permeability k_s played the role of a correction factor. The best agreement between the experimental and theoretical values of $T_0(t)$ was obtained at $k_s = 2.6\cdot10^{-12}$ m^2. The results of the calculations are shown in Fig. 2.

The largest disagreement between the theoretical and experimental data for nitrogen is seen at the beginning of the process, when the initial temperature of the specimen has a significant effect (see Fig. 2a with q_0 = 4382 W/m^2). This effect is not accounted for by the model, since the process was assumed to be quasisteady. The deviation of the theoretical results from the experimental results on the section corresponding to stabilized heat transfer decreases to 1%. The fairly large difference between the theory and experiment for hydrogen at q_0 = 4375 W/m^2 (Fig. 2b) is probably due to the fact that such a large thermal load destabilizes the planar sublimation front [1, 3], making the method of calculation inapplicable. The theoretical temperature $T_0(t)$ does in fact decrease markedly (Fig. 2b) at q_0 = 4375 W/m^2, which is an indication that the front is unstable [3].

3. Approximate Analytic Solution of the Equations. In order to explain several features of porous-sublimational cooling (see Parts 4 and 5) and perform a sufficiently general analysis of this process, it is desirable to obtain an analytic solution to system (1-3).

Considering [4] that

$$P_s(T) = \delta \exp\left(-\frac{\omega}{T}\right), \quad \delta = \text{const}, \tag{4}$$

for most cryogens and determining $\eta_2(T)$ from the Sutherland formula [3], we find that a change in T_ℓ is accompanied by a smaller change in the function $\Psi(T_\ell)$ on the right side of (2) than in the left side of (2). This makes it possible to assume that $\Psi(T_\ell) \approx \Psi(T_L) = \Psi_L$, and to obtain an approximate solution of Eq. (2) [3]

$$T_l = \frac{2\omega}{\ln(\delta^2/\varkappa)}, \quad \varkappa = P_L^2 + \frac{2q_0\Psi_L(L-l)}{\omega k_s}. \tag{5}$$

The temperature gradient along a porous body during porous-sublimational cooling is usually relatively small [3], i.e., $\lambda_s = \lambda_s(T) \approx \text{const}$. We then find from (3) that

$$T_0 = T_l + \frac{q_0 l}{\lambda_s}. \tag{6}$$

If $q_0 = \text{const}$, then it follows from (1) that

$$l(t) = L - \frac{q_0 t}{\rho_1 \varepsilon_s \varepsilon_d \gamma}. \tag{7}$$

Equations (5-7) give an approximate analytic solution to system (1-3). Comparison of the analytic and numerical [3] solutions of this system shows that the error of approximation (5-7) is no greater than several percent.

4. Nonmonotonicity of the Temperature Curves. In can be seen from Fig. 2 that given sufficiently large q_0, the curves $T_0 = T_0(t)$ are nonmonotonic. To find an explanation for this phenomenon, we will examine a process in which q_0 and P_L are constant. In this case, we can examine the function $T_0(\ell)$ instead of $T_0(t)$, since $T_0(t) = T_0[\ell(t)]$. Meanwhile, the function $\ell(t)$ is monotonic (see (1), (5-6)).

Let us find the minimum value $q_0 - \tilde{q}_0$ at which $T_0(\ell)$ can have an extremum. At the point of the extremum $\ell_0 = \ell_*$ we have $T_0'(\ell_*) = 0$ and we find from (5-6) that

$$\varkappa(q_*, l_*)\ln^2\left[\frac{\delta^2}{\varkappa(q_*, l_*)}\right] = \frac{4\lambda_s\Psi_L}{k_s}, \tag{8}$$

which gives the function $q_* = q_*(\ell_*)$. Differentiating (8) with respect to ℓ_* leads to

$$\left[\frac{1}{2}\ln\left(\frac{\delta^2}{\varkappa}\right) - 1\right][q_*'(l_*)(L-l_*) - q_*(l_*)] = 0. \tag{9}$$

It is obvious that $T_\ell \leq T_{tr}$, and it follows from (5) that $\ell n(\delta^2/\kappa)/2 \geq \omega/T_{tr} \gg 1$ (the last inequality is satisfied for most cryogens). Thus, the first factor in (9) is positive, while $q_*'(\ell_*) = q_*(\ell_*)/(L - \ell_*) \geq 0$. This means that a decrease in q_* is accompanied by a shift in the extremum of the function $T_0(\ell)$ in the direction of smaller ℓ_*, while the minimum value $\min q_* = \tilde{q}_0$ is reached at $\ell_* = 0$. Thus, we obtain the following equation for $\tilde{q}_0$ from (8)

$$\varkappa(\tilde{q}_0)\ln^2\left[\frac{\delta^2}{\varkappa(\tilde{q}_0)}\right] = \frac{4\lambda_s\Psi_L}{k_s}, \tag{10}$$

where $\varkappa(\tilde{q}_0) = P_L^2 + 2\tilde{q}_0\Psi_L L/(\omega k_s)$.

We will show that at $q_0 < \tilde{q}_0$ the value of $T_0(\ell)$ increases with a decrease in ℓ. It follows from (5-6) that the sign of $T_0'(\ell)$ is determined by the sign of the function $\phi(\kappa) = \kappa \ln^2(\delta^2/\kappa) - 4\lambda_s\Psi\psi_L/k_s$. When $q_0 < \tilde{q}_0$ and $\ell = 0$ we have (see (5)) $\kappa(q_0, 0) < \kappa(\tilde{q}_0, 0)$. Thus, $\kappa(q_0, \ell) < \kappa(\tilde{q}_0, 0)$, since κ decreases with an increase in ℓ. On the other hand $\phi'(\kappa) > 0$ and $\psi'(\kappa)$ decreases with a decrease in κ. Thus, $\psi[\kappa(q_0, \ell)] < \psi[\kappa(\tilde{q}_0, 0]$. However, in accordance with (10), $\psi[\kappa(\tilde{q}_0, 0)] = 0$, i.e., at $q_0 < \tilde{q}_0$ the functions $\psi(\kappa)$ and $T_0'(\ell)$ are negative, while the value of $T_0(t)$ increases over time as a result of an increase in t.

The results obtained above agree well with the experimental data. In fact, the temperature T_0 increases over time (Fig. 2) for sufficiently small q_0. At a certain critical value $q_0 = \tilde{q}_0$ we have $T_0'(\tau) = T_0'(\ell)|_{t=0} = 0$ (Fig. 2a for $q_0 = 4382$ W/m^2), while at $q_0 > \tilde{q}_0$ the function $T_0(\tau)$ has a maximum. This maximum shifts in the direction of smaller t with an increase in q_0. In the case of experiments with nitrogen for which $\omega = 828$ K, $\lambda_s \approx 100$

W/(m·K), $T_L \approx 50$ K, $k_s = 2.6 \cdot 10^{-12}$ m^2, L = 49 mm, solution of Eq. (10) gives $\tilde{q}_0 \approx 4.4$ kW/m^2. The latter value is very close to the experimental value $\tilde{q}_0 = 4.38$ kW/m^2 (Fig. 2a).

The following physical explanation of the nonmonotonicity of the temperature curves is consistent with the model proposed above. The second term in (6) decreases during cooling, since there is then also a decrease in the distance ℓ between the sublimation front and the surface being cooled. Conversely, the first term (the temperature of the front) increases, since there is also an increase in pressure at the front due to an increase in the thickness of the porous layer $\Delta h = L - \ell$ through which the vapor is removed. Thus, the temperature T_0 can either increase or decrease, and it will behave nonmonotonically when the parameters are related in a certain way ($q_0 > \tilde{q}_0$).

5. Heat-Transfer Coefficient. Figure 3 shows the time dependence of the heat-transfer coefficient

$$\alpha_0 = \frac{q_0}{T_0 - T_L} \tag{11}$$

in the sublimation of nitrogen and hydrogen in porous copper.

It can be seen from Fig. 3 that q_0 also increases when there is an increase in α_0. We will show that this phenomenon is a characteristic feature of porous-sublimational cooling. It follows from (5-7) and (11) that the sign of $\partial\alpha_0/\partial q_0$ coincides with the sign of the expression

$$A + T_l\left[1 - \frac{T_l}{\omega}\frac{B}{(P_L^2 + B)}\right] - T_L, \tag{12}$$

where

$$A = \frac{q_0^2 t}{\lambda_s \rho_1 \varepsilon_s \varepsilon_d \gamma},$$

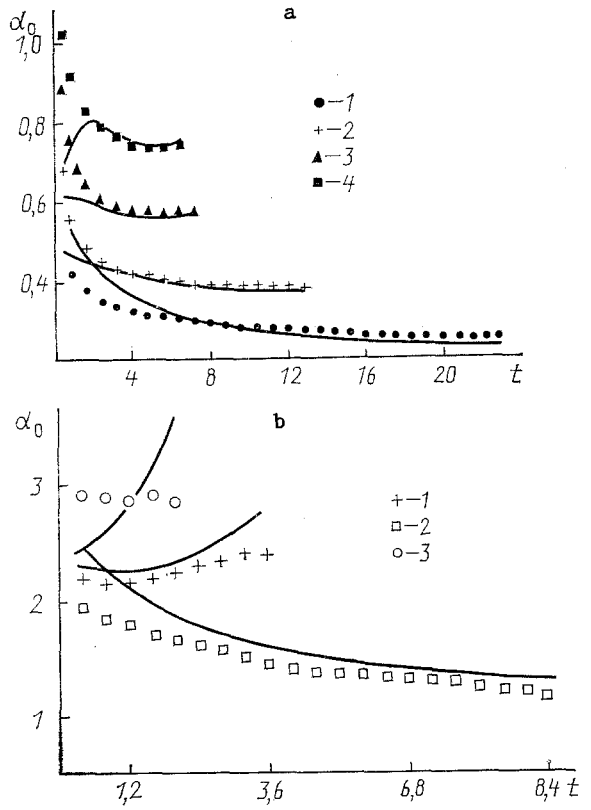

Fig. 3. Heat-transfer coefficient α_0 in relation to time t in the sublimation of nitrogen (a) and hydrogen (b) in porous copper: a: 1) $q_0 = 2447$ W/m^2; 2) 4382; 3) 6843; 4) 8300; b: 1) $q_0 = 1074$ W/m^2; 2) 2438; 3) 4375; the lines show the calculated results. α_0, kW/(m^2·K)

$$B = \frac{2A\lambda_s \Psi_L}{\omega k_s}.$$

If $t > 0$, then $A > 0$ and $B > 0$ and the second term in the brackets in (12) can be ignored – since $T_\ell/\omega \leq T_{tr}/\omega \ll 1$ (see Part 4). Because $T_\ell > T_L$ in this case, both Eq. (12) and the quantity $\partial\alpha_0/\partial q_0$ are positive, i.e., α_0 increases with an increase in q_0.

If the dependence of P_L on time is nonexistent (along with $T_L = T_s(P_L)$) or is the same for different q_0, then the curves $\alpha_0 = \alpha_0(t)$ corresponding to these values of q_0 do not intersect. If the curves do intersect, this means that for fixed t different values of q_0 correspond to identical α_0. The last result violates the condition $\partial\alpha_0/\partial q_0 > 0$. However, some of the curves in Fig. 3 do intersect. This has to do with the existence of the relation $P_L(t)$, which is different for different q_0. It should be noted that for the curves in Fig. 2 this effect is seen only at the beginning of sublimation, when the terms of (5) are of the same order. Over time, the second term in (5) rapidly increases and becomes appreciably greater than P_L, while the relation $P_L(t)$ can in general be ignored.

It follows from (11) that with fixed q_0 and T_L with sign of $\alpha_0'(t)$ is opposite that of $T_0'(t)$. If $q_0 < \tilde{q}_0$, then $T_0'(t) > 0$ (see Part 4), i.e., $\alpha_0'(t) < 0$. Thus, the maximum value of α_0 is reached at $t = 0$ ($\ell = L$) and the minimum value at $t = \tau$ ($\ell = 0$). Taking this into consideration, we use (4-6) and (11) to find that at $q_0 < \tilde{q}_0$

$$\max\alpha_0 = \frac{\lambda_s}{L}, \quad \min\alpha_0 = q_0\left\{2\omega \ln^{-1}\left[\frac{\delta^2}{P_L^2 + 2q_0\Psi_L L/(\omega k_s)}\right] - T_s(P_L)\right\}^{-1}.$$

CONCLUSIONS

1. A study was made of porous-sublimation cooling. During the process that was studied, heat was removed from the surface being cooled through a porous skeleton and transferred to a solid cryogen located in the pores of the skeleton.

2. The temperature of the cooled surface was measured and calculated for the sublimation of nitrogen and hydrogen in porous copper under different thermal loads. Good agreement was obtained between theory and experiment.

3. It was found experimentally that the temperature of the cooled surface changes nonmonotonically when surface heat flux exceeds a certain critical value. At heat fluxes sufficiently close to critical, this phenomenon is satisfactorily described by a mathematical model of the process. An equation was obtained to determine the critical heat flux.

4. An increase in the thermal load is accompanied by an increase in the heat-transfer coefficient for the cooled surface. An analysis of the equations that describe the process showed that this phenomenon is a characteristic feature of porous-sublimational cooling.

5. It was shown theoretically for the case of a constant heat flux and constant temperature on the evacuation surface that the temperature of the cooled surface increases over time and the heat-transfer coefficient decreases at heat fluxes below the critical value. Expressions determining the minimum and maximum heat-transfer coefficients were obtained for this case.

NOTATION

ρ, density; η, absolute viscosity; ε, porosity; k, permeability; λ, thermal conductivity; ε_d, fraction of pore space occupied by the solid cryogen; L, height of the porous body; ℓ, coordinate of the sublimation front; R, universal gas constant; τ, time of complete sublimation of the cryogen; μ, molecular weight; T, temperature; P, pressure; x, coordinate; t, time. Indices: 1, solid cryogen; 2, vapor; 3, material of the porous skeleton; o, surface being cooled; L, vapor evacuation surface; ℓ, sublimation front; s, porous skeleton or saturated state; tr, triple point.

LITERATURE CITED

1. S. M. Ostroumov, Inzh.-fiz. Zh., 59, No. 6, 910-916 (1990).
2. V. V. Druzhinets and N. M. Levchenko, "Experimental study of the efficiency of porous structures for low-temperature sublimational cooling," Preprint. No. 5-89, Fiz-Tekh. Inst. Niz. Temp. Akad. Nauk Ukr. SSR, Kharkov (1989).
3. S. M. Ostroumov, "Selection and optimization of parameters of porous-sublimational

cold accumulator," Preprint. No. 25-89, Fiz.-Tekh. Inst. Niz. Temp. Akad. Nauk Ukr. SSR, Kharkov (1989).
4. B. I. Verkin, V. F. Getmanets, and R. S. Mikhal'chenko, Thermophysics of Low-Temperature Sublimational Cooling [in Russian], Kiev (1980), pp. 80-84, pp. 115-122.
5. A. V. Alekseev, N. M. Levchenko, V. R. Litvinov, et al., "Automation of thermophysical experiments and complex tests of cryoturbogenerators with a computer," Preprint. No. 32-85, Fiz. Tekh. Inst. Niz. Temp. Akad. Nauk Ukr. SSR, Kharkov (1985).
6. I. S. Zhitomirskii and V. G. Romanenko, Inzh.-fiz. Zh., 57, No. 5, 864-865 (1989).

COMPARISON OF CONVECTIVE HEAT TRANSFER MODELS IN POROUS MEDIA

Yu. A. Zarubin

UDC 536.244

A comparison of experimental data with theory has shown the applicability of both the one-temperature and the two-temperature models of convective heat transfer in porous media.

The temperature field in a porous medium, formed as a result of convective transfer, often governs the intensity of the physical and chemical processes occurring in the equipment of heterogeneous catalysis, in heat exchangers, in oil and watering bearing deposits and so on. The main physical phenomena caused by the temperature distribution in a porous medium are convective heat transfer, the heat conduction of the porous medium skeleton and heat transfer agent, the heat transfer between them, the dispersion of the flow of heat transfer agent in the porous medium, heat transfer with the surrounding medium, and the action of heat sources and sinks. It is extremely complicated to analyze a universal mathematical model because the factors are diverse and the coefficients entering into the model are uncertain. It is therefore important to identify the important factors and to study the possible use of simplified models accounting for a limited number of factors and providing reliable heat calculations, at least at an engineering level.

The model of convective heat transfer in porous media, accounting for heat conduction of the phases and interphase heat transfer and with no heat sources, can be formulated in the form based on the method of the ensemble average, e.g., in [1, 2]:

$$\operatorname{grad} q_{i,i} + \operatorname{div}(m_i v_i \rho_i c_i) + \frac{\partial}{\partial \tau}(m_i \rho_i c_i) = \sum_{j=i}^{n} q_{ij}, \quad i = \overline{1, n}. \tag{1}$$

In addition, we evidently have the relations $\Sigma m_i = 1$, $q_{ij} = -q_{ji}$, and for the skeleton of the porous medium we have ($i = 1$) $v_1 = 0$.

It is important that the heat flux due to conduction of the phases for the porous medium skeleton must be determined with allowance for the thermal resistances at the points of contact of the grains, and for the liquid and gaseous phases one must allow for the component due to dispersion of the flow because of multiphase motion, inhomogeneity of the porous channels, and the presence of a velocity distribution inside an individual pore channel. To allow for these phenomena analytically is extremely complex, and this leads to the use of simplified models in which the transfer coefficients (heat conduction and interphase heat transfer) are in the nature of effective values and are determined from results of natural modeling. The widest use has been made of the one-temperature model, which postulates that the temperatures of the porous medium skeleton and the heat transfer agent are the same. Accordingly, the intensity of deformations of the temperature field are determined by the value of a single effective thermal conductivity. Models which account for interphase heat transfer are customarily studied [3, 4] with the assumption that one can

The Ivan-Frankovskii Institute of Oil and Gas. Translated from Inzhenerno-fizicheskii Zhurnal, Vol. 60, No. 5, pp. 754-758, May, 1991. Original article submitted March 29, 1990.

 0022-0841/91/6005-0572$12.50